J Comput Aided Mol Des (2014) 28:751–763
DOI 10.1007/s10822-014-9756-9

Molecular insight of isotypes specific β-tubulin interaction of tubulin heterodimer with noscapinoids

Seneha Santoshi · Pradeep K. Naik

Received: 18 December 2013 / Accepted: 23 May 2014 / Published online: 11 June 2014

Abstract Noscapine and its derivatives bind stoichiometrically to tubulin, alter its dynamic instability and thus effectively inhibit the cellular proliferation of a wide variety of cancer cells including many drug-resistant variants. The tubulin molecule is composed of α- and β-tubulin, which exist as various isotypes whose distribution and drug-binding properties are significantly different. Although the noscapinoids bind to a site overlapping with colchicine, their interaction is more biased towards β-tubulin. In fact, their precise interaction and binding affinity with specific isotypes of β-tubulin in the αβ-heterodimer has never been addressed. In this study, the binding affinity of a panel of noscapinoids with each type of tubulin was investigated computationally. We found that the binding score of a specific noscapinoid with each type of tubulin isotype is different. Specifically, amino-noscapine has the highest binding score of −6.4, −7.2, −7.4 and −7.3 kcal/mol with $\alpha\beta_{I}$, $\alpha\beta_{II}$, $\alpha\beta_{III}$ and $\alpha\beta_{IV}$ isotypes, respectively. Similarly **10** showed higher binding affinity of −6.8 kcal/mol with $\alpha\beta_{V}$, whereas **8** had the highest binding affinity of −7.2, −7.1 and −7.2 kcal/mol, respectively with $\alpha\beta_{VI}$, $\alpha\beta_{VII}$ and $\alpha\beta_{VIII}$ isotypes. More importantly, both amino-noscapine and its clinical derivative, bromo-noscapine have the highest binding affinity of −46.2 and −38.1 kcal/mol against $\alpha\beta_{III}$ (overexpression of $\alpha\beta_{III}$ has been associated with resistance to a wide range of chemotherapeutic drugs for several human malignancies) as measured using MM-PBSA. Knowledge of the isotype specificity of the noscapinoids may allow for development of novel therapeutic agents based on this class of drugs.

Keywords Noscapinoids · Tubulin · Isotypes · Binding affinity · MD simulation

Introduction

Microtubules are highly dynamic cytoskeletal polymers composed of α- and β- tubulin heterodimers that regulate various physiological functions such as cell division, maintain intracellular transport, positioning of cellular organelles and cellular motility [1]. The crucial roles microtubules play in cell division, the segregation of chromosomes, make them an attractive target for cancer chemotherapy. A number of tubulin-binding molecules with antimitotic properties such as taxanes, vinca alkaloids and podophyllotoxin have been discovered in recent years [2–4]. Tubulin is encoded by multiple genes that represent multiple isotypes of α- and β-tubulin that are expressed in a tissue specific manner [5, 6]. Cancerous cells disregulate this tissue-specific pattern; particularly β_{III} overexpression has been associated with aggressive drug resistant cancer cells [7–10]. Other isotypes are also disregulated in cancerous cells in comparison to noncancerous cells [5, 6, 11–13].

Recent reports suggest that differential expression of α- and β-tubulin isotypes by mammalian tissues results in

Electronic supplementary material The online version of this article (doi:10.1007/s10822-014-9756-9) contains supplementary material, which is available to authorized users.

S. Santoshi · P. K. Naik (✉)
Department of Biotechnology and Bioinformatics, Jaypee University of Information Technology, Waknaghat, Distt., Solan 173 234, Himachal Pradesh, India
e-mail: pknaik1973@gmail.com; pradeep.naik@juit.ac.in

Present Address:
P. K. Naik
Department of Biotechnology, Guru Ghasidas Vishwavidyalaya, A Central University, Koni, Bilaspur 495 009, Chhattisgarh, India

differential binding affinities of antimitoic agents [14]. Varied expression of tubulin isotypes also affects the sensitivity of cancer cells of different tissue origin to the tubulin binding agents. Although current antitubulin drugs bind to all of these isotypes, they showed better responses against specific types of cancer cells that are overexpressing a particular type of isotype [12, 14]. Moreover, overexpression of some isotypes in cancer cells has been linked to resistance towards antimitotic drugs [12, 14, 15]. As an example overexpression of β_{III} in cancer cells such as ovarian, breast and non-small-cell lung cancer has been linked to resistance to paclitaxel [7–10]. Similarly overexpression of class β_V in cancer cells also leads to resistance to taxane-based chemotherapy [15]. Therefore it is of utmost importance to design tubulin binding drugs that can bind ubiquitously onto different tubulin isotypes and are lethal to cancer cells but not to normal cells. Screening for similar new microtubule-targeting agents that possess functional groups similar to colchicine and podophyllotoxin led to discovery of noscapine that binds to the tubulin heterodimer and perturbs the secondary conformation of tubulin, as a result leading to mitotic arrest. Noscapine has been used historically as an anti-cough medicine, and is currently in Phase I/II clinical trials as an anticancer drug. However, unlike the majority of the microtubule-targeting agents, noscapine does not significantly alter the ability of tubulin to form microtubules [16]. Investigating the mechanism behind this discrepancy, it was found that noscapine arrests cancer cells by altering the dynamic instability of microtubules, primarily by increasing the time spent in the attenuated states of dynamic instability [17–20]. Also it was observed that cancer cells of different tissue origin that have altered expression of β-tubulin isotypes are differentially sensitive to these tubulin binding agents [21–24]. Moreover, noscapine can efficiently inhibit paclitaxel resistant human ovarian cancer cells (1A9PTX10 and 1A9PTX22) that possess a mutation in β-tubulin [25]. A number of noscapine analogs have been reported in recent years as having superior efficacy in regard to inhibition of cancer cell proliferation, while having negligible effects on normal cells [17, 18, 21–24]. Furthermore, owing to its relatively non-toxic and safe profile, we have rationally designed many derivatives of noscapine with enhanced tubulin binding affinity [26, 27].

Noscapine and its derivatives bind to a site at the interface of α- and β-tubulin but are more biased to β-tubulin, [28]. Thus any substitution or changes in amino acids on and near the binding site of noscapinoids that exists in β-tubulin would significantly affect the binding affinity and responses of noscapine derivatives. Of particular interest in this manuscript we have made an effort to investigate the mechanistic details of differential activity of noscapinoids across cancer types that are reported to have different proportions of β-tubulin isotypes. Towards this end, we have used noscapine and some of its derivatives for the computational analysis of binding interaction with tubulin heterodimers made up of α- and isotype-specific β-tubulin. Contrastingly different isotypes of α-tubulin are also reported. However, the comparative analysis of isotypes of α-tubulin did not reveal any mismatches in the amino acids present in or near (within 12 Å) of the noscapinoids binding site. Hence the α-tubulin isotypes are not considered in this study. Furthermore, binding of noscapinoids is more biased towards β-tubulin whereas the α-tubulin contributes very little in the binding. Understanding of molecular interactions of these agents with tubulin isotypes would be important to improve the efficacy of noscapinoids towards specific cancer types.

Materials and methods

Isotypes of β-tubulin and sequence analysis

To investigate the binding affinity of noscapine and its derivatives onto isotype-specific β-tubulin, we have constructed tubulin heterodimers comprised of α-tubulin and different isotypes of β-tubulin. The protein sequences of eight human β-tubulin isotypes [β_I to β_{VIII}] reported previously were downloaded from the NCBI database. The representative sequences of β-isotypes: β_I (gi:18088719), β_{II} (gi:29788768), β_{III} (gi: 1297274), β_{IV} (gi: 135470), β_V (gi:14201536), β_{VI} (gi: 62903515), β_{VII} (gi:1857526) and β_{VIII} (gi:42558279) were used to build tubulin heterodimers. These sequences of β-tubulin isotypes were aligned and compared using a multiple sequence alignment program (Bioedit version 7.1.9) [29].

Template preparation and homology modeling of tubulin isotypes

The co-crystallized structure of the colchicine-tubulin complex (PDB ID: 1SA0, resolution 3.58 Å) was used as a template for homology modeling of tubulin isotypes. In the crystal structure of 1SA0, some of the amino acids such as 37–47 (α-tubulin) and 275–284 (β-tubulin) were found to be missing and these gaps were filled by homology modeling based on PDB ID: 3DU7 (C-chain) and PDB ID: 3RYC (D-chain) respectively as templates using Prime (version 3.0, Schrödinger). The structure obtained was energy minimized using OPLS 2005 force field with Polak-Ribiere Conjugate Gradient (PRCG) algorithm, which was stopped either after 5,000 steps or after the energy gradient converged below 0.001 kcal/mol using Macromodel (version 9.9, Schrödinger). The structure was further refined by performing an all atom molecular dynamics (MD)

simulation in explicit water using GROMACS 4.5.4 software [30] and the GROMOS96 force field on a time scale of 10 ns. By enclosing the molecule in a dodecahedron solvated with the SPC216 water model provided in the GROMACS package, three-dimensional periodic boundary conditions were imposed and the structure was energy minimized using 1,000 steps of steepest descent minimization. To achieve electro-neutrality, 32 Na^+ counter ions were added to the system and the results locally minimized using 100 steps of steepest descent. The electrostatic term was described using the Particle Mesh Ewald algorithm [31]. For the calculation of the coulombic and van der Waals interactions at 1.0 nm, the LINCS [32] algorithm was used to constrain all bond lengths and cut-off distances. At 300 K and normal pressure we equilibrated the system by 100 ps of MD runs with position restraints on the protein to allow the relaxation of the solvent molecules. With a coupling time of 0.1 ps at the default setting, the system was coupled to the external bath by the Berendsen thermostat. The final MD calculations were performed for 10 ns with a time step of 2 fs. A total of 5,000 frames were generated in the MD trajectories, out of which the last 2,000 frames were used to generate an average structure of the tubulin. The overall quality of the model, stereochemical values and non-bonded interactions were evaluated using PROCHECK [33, 34], ERRAT [35] and VERIFY3D [36].

The homology models of different tubulin isotypes were built based on the above prepared and refined structure of tubulin (PDB ID:1SA0) as template using Prime [version 3.0, Schrödinger. Furthermore, the modeled structures were refined by performing an all atom MD simulation of 10 ns as described previously. The quality of the modeled structures of tubulin isotypes were evaluated using PROCHECK, ERRAT and VERIFY3D.

Ligand preparation

Molecular structures of noscapine and its derivatives (Fig. 1) that had been previously demonstrated to be tubulin binding agents [17, 18, 21–24, 26, 27] were built using the molecular builder of Maestro (version 9.2, Schrödinger). All these structures were energy minimized using Macromodel (version 9.9, Schrödinger) and OPLS 2005 force field with PRCG algorithm (1,000 steps of minimization and an energy gradient of 0.001). Appropriate bond order for each structure was assigned using Ligprep (version 2.5, Schrödinger). Furthermore, these molecular structures were geometrically optimized using hybrid density functional theory with Becke's three-parameter exchange potential and the Lee–Yang–Parr correlation functional (B3LYP) [37, 38] with basis set 3-21G* [39–41]. Jaguar (version 7.7, Schrödinger, LLC) was used for the geometrical optimization of the ligands.

Prediction and analysis of noscapinoid binding pocket

Different binding sites were predicted and analyzed for the modeled αβ-tubulin isotypes using SiteMap (version 2.4, Schrodinger). However, only the noscapinoid binding site [28] (at the interface between α- and β-tubulin) for each protein structure which is in agreement with the predicted noscapinoid binding site and partially supported by experimental study [28] was selected for comparative analysis and predicting the binding affinity of noscapinoids. The best way to understand the noscapinoid binding site is to obtain a co-crystal structure with tubulin, which is not yet possible so far. Alternatively, only one piece of experimental evidence (competition interaction of Br-noscapine with colchicine binding) is so far reported that revealed a binding site of noscapinoid at or near the colchicine binding site of tubulin [28]. The binding site residues (comprised of 16 amino acids) which are in agreement with the predicted noscapinoids binding site [28] from each of the tubulin isotypes were extracted and superimposed for comparative analysis.

Molecular docking of ligands

Molecular docking of noscapinoids (Fig. 1) onto tubulin isotypes was performed using "Extra Precision" (XP) algorithm of Glide docking (version 5.7, Schrödinger) [42, 43]. The noscapinoid binding pocket on different αβ-tubulin isotypes was defined using a concentric grid box at the centroid of the noscapinoid binding site using the Glide grid-receptor generation program. A bounding box of size 12 Å × 12 Å × 12 Å was defined in order to confine the mass center of the docked ligand. The larger enclosing box of size 12 Å × 12 Å × 12 Å was also chosen so that it occupied all the atoms of the docked poses. All the ligands were then docked into the binding site using Glide XP (extra precision) and evaluated using a Glide XP_{Score} function. For the ligand docking stage, a scale factor of 0.4 for van der Waals radii was applied to atoms of protein with absolute partial charges less than or equal to 0.25. Out of the 10,000 poses that were sampled, 1,000 were taken through minimization (conjugate gradient) and the 30 structures having the lowest energy conformations were further evaluated for a favorable Glide docking score. The single best conformation for each ligand was considered for further analysis. The residues within 12 Å of the docked ligands were extracted and analyzed for differences in molecular interactions with respect to tubulin isotypes.

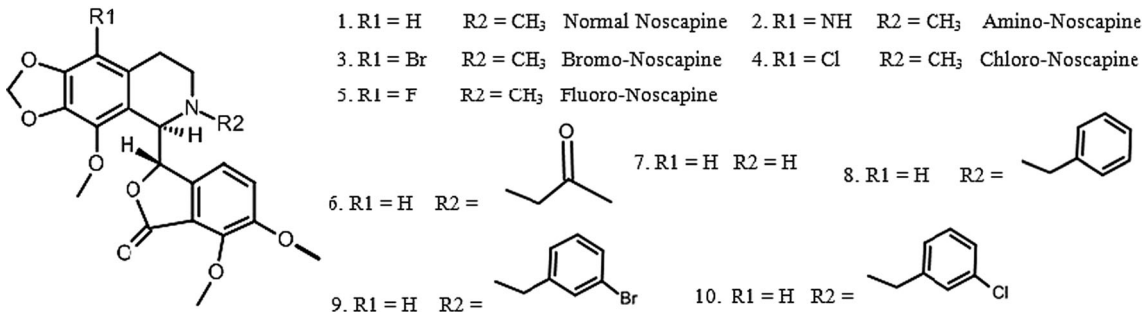

Fig. 1 Chemical structure of noscapine and its derivatives used in the study. These derivatives were previously demonstrated to be tubulin binding agents

Molecular dynamics simulations of the docked complexes

To specifically investigate the binding affinity of amino-noscapine (the most potent derivative in our library), bromo-noscapine (the clinical derivative) and noscapine (the lead molecule) onto the $\alpha\beta_{III}$ isotype, we calculated their binding free energy. To achieve this, the complex of $\alpha\beta_{II}$ isotype with amino-noscapine, bromo-noscapine and noscapine, obtained after Glide docking was used as an initial conformation for MD simulation. The MD simulation was performed in AMBER 11.0 [44] software suite and the force fields used were AMBER ff99SB [45] for the protein and general AMBER (GAFF) [46] for the ligands. To solvate the system, TIP3P water model was used in an octahedral box with a distance of 15 Å between the wall of the box and the closest atom of the complex. To neutralize the system 31 Na^+ ions were added as counter ions. The molecular systems were first energy minimized with 500 steps of steepest descent energy minimization, followed by 500 steps of conjugate gradient energy minimization so as to remove the bad contacts in the crystal structure; this was done in 3 consecutive rounds. With the force constants of 10 and 2 $kcal^{-1}$ $Å^{-2}$ respectively, positional restraints were applied to the whole system for the first and second round to allow for relaxation of the solvent molecules. In the third round the whole system was minimized without restraint. Finally a 10 ns MD simulation was carried out following 200 ps of equilibration at 300 K. With a time step of 2 fs a total of 5,000 frames were generated. SHAKE algorithm [47] was applied for all the bonds involving hydrogen bonds. The non-bonded cut off distance was 10 Å. The particle mesh Ewald (PME) method was applied to treat long-range electrostatics interactions. The temperature of the system was regulated using the langevin thermostat. All equilibration and subsequent MD stages were carried out in an isothermal isobaric (NPT) ensemble using a Berendsen barometer [47–49] with a target pressure of 1 bar, recording trajectories every 2 ps.

Calculation of binding free energy

We have used molecular mechanics generalized Born surface area (MM-GBSA) and molecular mechanics Poisson Boltzmann (MM-PBSA) [50] to calculate the binding free energy implemented in AMBER 11.0. For this calculation a total of 1,000 snapshots generated from the last 2 ns of the MD trajectory for each molecular species were considered. The binding free energy was computed as the difference between the energy of the complex with the combination energy of the receptor and ligand for each frame for a total of 1,000 frames that were generated. The binding free energy was then calculated for each molecular species as

$$\Delta G_{bind} = G_{complex} - \left(G_{receptor} + G_{ligand}\right).$$

The free energy, G for each species was calculated by the following scheme using the MM-PBSA and MM-GBSA methods [50–53].

$$G = E_{gas} + G_{sol} - TS$$

$$E_{gas} = E_{int} + E_{ele} + E_{vdw}$$

$$G_{ele,PB(GB)} = E_{ele} + G_{PB(GB)}$$

$$G_{sol} = G_{sol-np} + G_{PB(GB)}$$

$$G_{sol-np} = \gamma SAS$$

Here, E_{gas} is the gas-phase energy; E_{int} is the internal energy; E_{ele} and E_{vdw} are the coulomb and van der Walls energies, respectively. E_{gas} was calculated using the ff99SB molecular mechanics force field. G_{sol} is the solvation free energy and can be split into polar and non-polar contributions. $G_{PB(GB)}$ is the polar solvation contribution calculated by solving the GB and PB equations. $G_{ele,\,PB(GB)}$ is the polar interaction contribution. $G_{sol\text{-}np}$ is the nonpolar solvation contribution and was estimated via the solvent-accessible surface area (SAS), which was determined using a water probe radius of 1.4 Å. T and S are the temperature and the total solute entropy, respectively.

Per residue energy contribution with ligands

To achieve the detailed view of the $\alpha\beta_{III}$ isotype and noscapinoids interaction, we computed the binding free-energy contribution of each residue using the MM-GBSA model. The binding energy of each ligand-residue pair includes three energy terms: the van der Waals contribution (δE_{vdw}), the electrostatic contribution (δE_{ele}) and the solvation contribution (δE_{sol}). All the energy components were calculated using the same frames obtained from MD trajectories that were used for calculation of binding free energy. The contribution of each residue to the binding free energy was obtained by summing up the contribution of each atom of the given residue.

Results and discussion

Sequence analysis of isotype specific β-tubulin

Different isotypes of β-tubulin (β_I–β_{VIII}) encoded by different genes exhibited tissue restricted expression patterns. Cancer cells especially express a variety of isotypes and are not limited to the isotypes that are expressed in non-cancerous cells from which they are derived. To illustrate this, β_{II} was over-expressed in leukemia and Hodgkin's lymphoma [12]; whereas, the HeLa cell line shows maximum expression of β_I with a little expression of β_{III} and even less expression of β_{II} and β_{IV} [14]. Similarly both A549 and CEM cell lines over-express β_{III}, while β_{II} is overexpress in comparison to all other β-tubulin isotypes in the MCF-7 cell line [14].

The protein sequences of eight human β-tubulin isotypes (β_I–β_{VIII}) reported previously [12] were downloaded from the NCBI database. The representative sequences of each isotype were compared by multiple sequence alignment using bioedit. The sequences were observed to have mismatches at different positions with an identity score ranging from 77 to 94 (Fig. 2). In particular the mismatches were mostly concentrated in the region of residues 160–370 that constitutes the noscapinoid binding site [28]. No clear consensus in amino acid was observed at four different positions (236, 239, 315, 316, 351 and 368) within the noscapinoid binding site with reference to the crystal structure of αβ-tubulin (PDB ID: 1SA0) (Table 1). As an example, Ala315 is substituted by Threonine in both β_{III} and β_V as well as Cysteine in β_{VI}, whereas Val316 is substituted by Isoleucine in β_{II} and β_{VI} to β_{VIII} (Table 1). Furthermore, the sequence analysis of the amino acids within 12 Å of the noscapinoid binding pocket also reveals many differences in and near the binding site (Fig. 2). Differences in binding site residues among αβ-tubulin isotypes may contribute to differences in binding energy with noscapinoids.

Homology modeling of αβ-tubulin isotypes

The x-ray crystal structures of tubulin heterodimers composed of α- and isotypes specific β-tubulin are not available. Thus, it is necessary to build these structures for comparative analyses. We have used the crystal structure of tubulin (PDB ID: 1SA0) as a template for the homology modeling. The missing amino acids in the template structure were filled in using homology model building and the structure was further refined using MD simulation. An ERRAT score of 88.4 and a VERIFY 3D score of 95.3 % indicated a good quality structure for the template. The PROCHECK results also showed 94.8 % of backbone angles were in allowed regions with G-factors of −0.12. Ramachandran plot analysis revealed only 1.6 % of residues in the disallowed region and 2.3 % of residues in generously allowed regions. Thus the overall quality of the template structure was very good for homology modeling of αβ-tubulin isotypes. The molecular structures of these αβ-tubulin isotypes were built based on the prepared template structure and further refined using an MD simulation run of 10 ns. The equilibration of the MD trajectories was monitored based on the convergence of plots of root-mean-square deviations (RMSDs) of Cα carbon atoms of αβ-tubulin isotypes during 10 ns of MD simulation starting from the initial modeled structure (Supplementary Figure S1). The relative fluctuation in the RMSD of the Cα atoms was found to be very small after the initial equilibration (∼5 ns), demonstrating the convergence of the simulation. A total of 5,000 frames were generated out of which the last 2,000 frames were used to generate an average structure of the αβ-tubulin isotypes. These modeled structures were of good quality with the ERRAT scores ranging from 88 to 95 and VERIFY 3D score within 97–99 %. The Ramachandran plot analysis also revealed good quality structures with the percentage of residues in disallowed regions ranging from only 1.2 to 1.6 %. The modeled αβ-tubulin isotypes showed significant structural similarity with the template protein (1SA0) with an RMSD value in the range of 1.08–1.25 Å (Supplementary Figure S2). However, pairwise comparative analysis of these αβ-tubulin isotypes showed RMSD values in the range of 0.96–1.51 Å (Supplementary Table 1).

Computational analysis of noscapinoid binding site

To ascertain the impact of the structural differences among the αβ-tubulin isotypes on their noscapinoid binding site, we did a comparative analysis. In the absence of co-crystal structure of noscapinoid with tubulin, the noscapinoid binding site which is in agreement with the Joshi et al. [28] from different αβ-tubulin isotypes was characterized using Sitemap based on various physico-chemical properties and

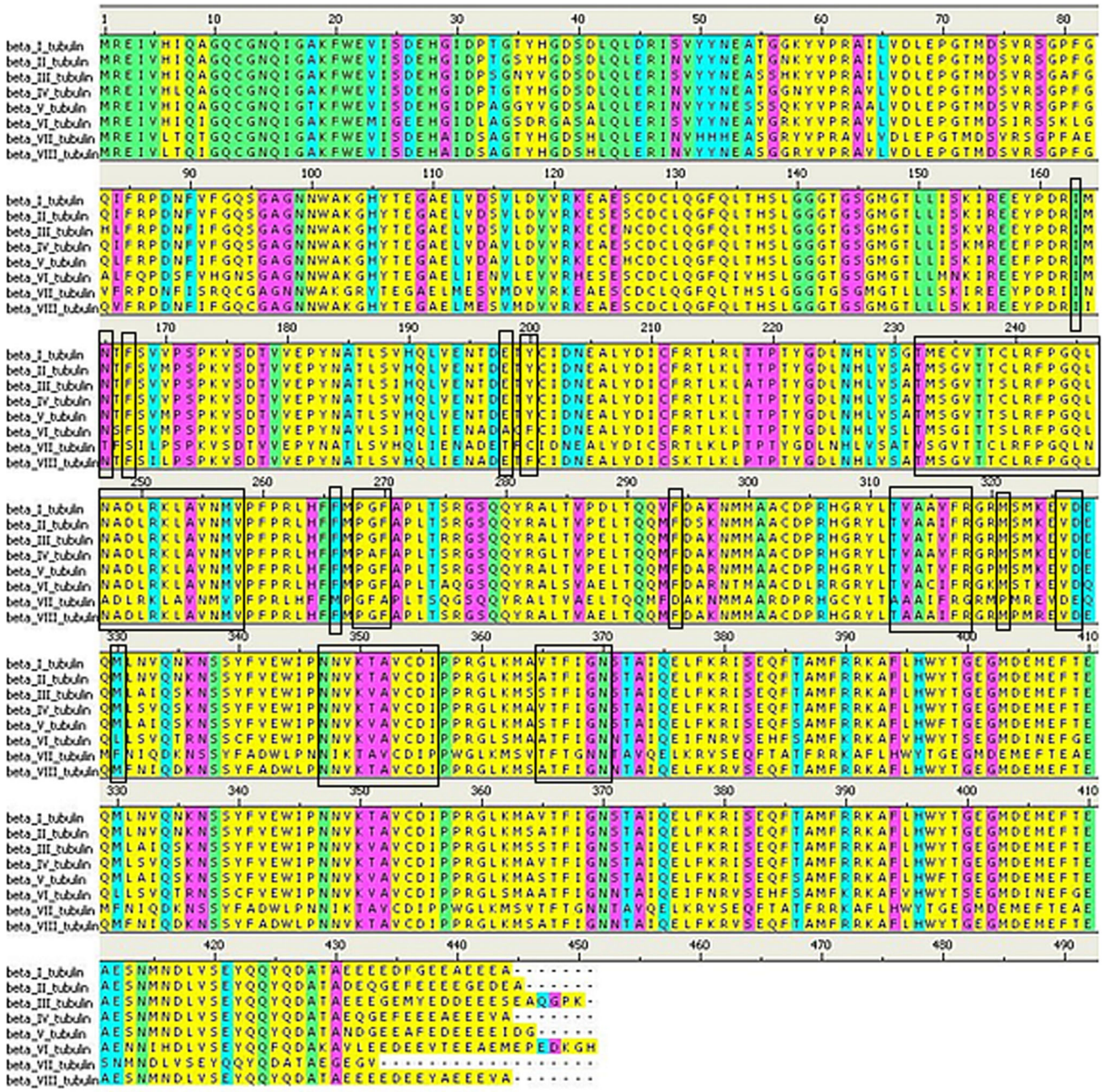

Fig. 2 Multiple sequence alignment of β_I–β_{VIII} isotypes showing mismatches at certain places. All the isotypes are comprised of different lengths of amino acid sequences. *Green colour* represents identical residues, *cyan* represents strongly similar, *pink* represents weakly similar and *yellow* represents very strongly dissimilar residues. The amino acids located in or near 12.0 Å of the noscapinoid binding site (marked in the *boxes*) show mismatches at certain places

included in Supplementary Table 2. The sitemap scores for all the αβ-tubulin isotypes ranging from 0.58 ($\alpha\beta_I$) to 0.82 ($\alpha\beta_{II}$) suggest an overall better accommodation of the noscapinoids within the binding site. However, due to various substitutions of amino acids within the binding site region, differences in various parameters among the isotypes were noticed. Similarly, the binding sites among the αβ-tubulin isotypes also differed in their ability to accommodate the solvent molecules as measured by exposure and enclosure scores. Apropos to this finding, the binding affinity of the noscapinoids may differ with different αβ-tubulin isotypes. All-vs-all comparison of the amino acids within 12 Å of binding site, measured by RMSD score, showed significant variations among the isotypes (Supplementary Table 3). The RMSD score was found to be maximum between $\alpha\beta_I$–$\alpha\beta_{VI}$, $\alpha\beta_{VI}$–$\alpha\beta_V$ and

Table 1 Mismatches in amino acids comprising the noscapinoid binding site [28] among different β isotypes in comparison to the template (1SA0)

Isotype	Amino acid position															
	179 [A]	235	236	237	239	246	248	252	253	314	315	316	350	351	366	368
1SA0	Thr	Gly	Val	Thr	Cys	Leu	Ala	Lys	Leu	Ala	Ala	Val	Lys	Thr	Thr	Ile
β_I	Thr	Gly	Val	Thr	Cys	Leu	Ala	Lys	Leu	Ala	Ala	Val	Lys	Thr	Thr	Ile
β_{II}	Thr	Gly	Val	Thr	Cys	Leu	Ala	Lys	Leu	Ala	Ala	**Ile**	Lys	Thr	Thr	Ile
β_{III}	Thr	Gly	Val	Thr	**Ser**	Leu	Ala	Lys	Leu	Ala	**Thr**	Val	Lys	**Val**	Thr	Ile
β_{IV}	Thr	Gly	Val	Thr	Cys	Leu	Ala	Lys	Leu	Ala	Ala	Val	Lys	Thr	Thr	Ile
β_V	Thr	Gly	Val	Thr	**Ser**	Leu	Ala	Lys	Leu	Ala	**Thr**	Val	Lys	**Val**	Thr	Ile
β_{VI}	Thr	Gly	**Ile**	Thr	**Ser**	Leu	Ala	Lys	Leu	Ala	**Cys**	**Ile**	Lys	**Val**	Thr	Ile
β_{VII}	Thr	Gly	Val	Thr	Cys	Leu	Ala	Lys	Leu	Ala	Ala	**Ile**	Lys	Thr	Thr	**Thr**
β_{VIII}	Thr	Gly	Val	Thr	Cys	Leu	Ala	Lys	Leu	Ala	Ala	**Ile**	Lys	Thr	Thr	Ile

There are six positions (highlighted in bold) where there are no clear consensuses in residues over all the β-isotypes

$\alpha\beta_{VI}$–$\alpha\beta_{VII}$ with values of 1.34, 1.35 and 1.35 Å, respectively. However, the binding site between $\alpha\beta_{II}$ and $\alpha\beta_{VIII}$ showed minimum differences with an RMSD of 0.66 Å. Furthermore, the noscapinoid binding sites, consisting of 16 amino acids [28], revealed significant differences as shown in Fig. 3. The differences in conformation and composition of binding sites among αβ-tubulin isotypes suggested differences in the overall environment of the binding site that may affect the binding affinity of noscapinoids.

Binding affinity of noscapinoids to different tubulin isotypes

To determine the binding affinity of noscapinoids at the noscapinoid binding site among different αβ-tubulin isotypes we have docked the lead molecule, noscapine as well as a set of biologically more active derivatives of noscapine, **1–10** using Glide-XP docking. The Glide docking program validates different positions, orientations and conformations of ligands in the receptor binding site in a systematic manner and returns the best docked poses of various ligands in the binding pocket. All the noscapinoids showed significant differences in binding score (Table 2) with respect to different αβ-tubulin isotypes. Moreover, the binding affinity of a specific noscapinoid was also found to be different with respect to different αβ-tubulin isotypes. As an example, amino-noscapine **(2)** showed the highest binding scores of −6.4, −7.2, −7.4 and −7.3 kcal/mol with $\alpha\beta_I$, $\alpha\beta_{II}$, $\alpha\beta_{III}$ and $\alpha\beta_{IV}$, respectively in comparison to the rest of the compounds. Similarly **10** showed the highest binding affinity of all the noscapinoids of −6.8 kcal/mol against $\alpha\beta_V$. Moreover, **8** showed highest binding affinities of −7.2, −7.1 and −7.2 kcal/mol, respectively against $\alpha\beta_{VI}$, $\alpha\beta_{VII}$ and $\alpha\beta_{VIII}$. The simplest reason could be the differences in binding mode of the noscapinoids among different isotypes mainly because of the differences in binding site amino acids. In a representative example, analysis of the binding mode of amino-noscapine across various αβ-tubulin isotypes revealed variation in hydrogen bonding (H-bond) patterns within the binding pocket of different αβ-tubulin isotypes from docked poses (Fig. 4). Only one H-bond is formed between the amino-noscapine and SerA(α-chain)178 in the binding pocket of $\alpha\beta_I$, $\alpha\beta_{IV}$ and $\alpha\beta_{VII}$. In contrast SerA178 forms two H-bonds with amino-noscapine in the binding pocket of $\alpha\beta_{II}$. Similarly amino-noscapine forms only one H-bond with ValB236 in the binding pocket of $\alpha\beta_{III}$; three H-bonds with AlaB248, SerA178 and LysB(β-chain)252 in the binding pocket of $\alpha\beta_{VI}$ as well as three H-bonds with SerA178, LysB252 and GlnA11 in the binding pocket of $\alpha\beta_{VIII}$. To gain more information about the interaction of noscapinoids with all the αβ-tubulin isotypes, we have calculated the per residue van der Walls (E_{vdw}) and electrostatic (E_{ele}) energy contribution of the residues within 12 Å of docked ligands. In a representative example with amino-noscapine (Supplementary Figure S3) the binding site amino acids showed significant contributions to the E_{vdw} and E_{ele} energy across all the αβ-tubulin isotypes. Specifically two amino acids, GluA198 and AspB249 of all the 8 αβ isotypes (except $\alpha\beta_{VI}$) have an appreciable E_{vdw} energy contribution (≤ -10 kcal/mol) with the binding of amino-noscapine. Similarly, the binding site residues of different αβ isotypes also contributed different E_{ele} energy with amino-noscapine (Supplementary Figure S3). The differences in the energy contribution among different isotypes can be explained as a result of substitution of amino acids of one kind by the other in and near the binding pocket. The differential binding affinity and mode of interaction of noscapinoids suggests different specificity of noscapinoids across different αβ-tubulin isotypes. This might be the reason that cancer cells of different tissue of

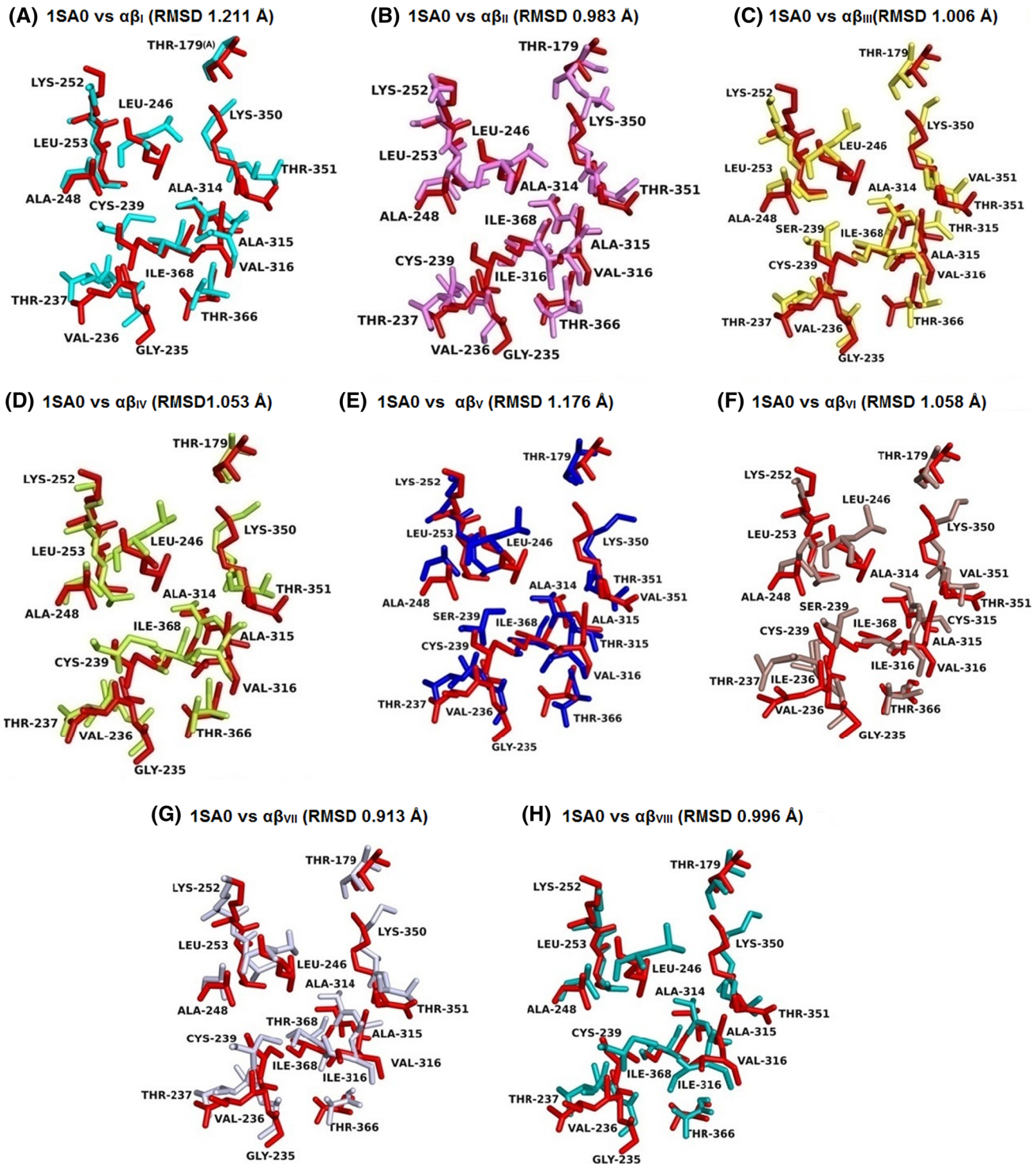

Fig. 3 Superimposition of the noscapinoid binding site [28] of the template structure (1SA0) in *red* and all the 8 isotypes of tubulin ($\alpha\beta_{I-VIII}$) represented in *different colours*. The figure clearly shows the differences between the binding sites of the isotypes due to changes in residues at different positions. The differences in conformation and composition of binding sites of different αβ-tubulin isotypes with the template structure suggested differences in the overall environment of the binding site that may affect the binding affinity of noscapinoids with these isotypes

origin show different sensitivities to noscapinoids as reported previously using NCI 60 cell lines [18, 21, 22, 24]. It should also be noted that these cell lines overexpress some isotypes. As an example, both A549 and CEM cell lines overexpress β_{III}, while β_{II} is overexpress in the MCF-7 cell line in comparison to all other β-tubulin isotypes

[14]. Recently also we have shown that all the 10 noscapine derivatives used in this study for computational study have different IC_{50} values for inhibition of cell proliferation among cell lines of different tissue of origin (such as Hela, MCF-7, CEM and A549) [27]. These results suggest that the reason for differential activity of noscapinoids against different cancer cell types may also be because of the differential expression of β-tubulin isotypes.

$\alpha\beta_{III}$ isotype as a potential target for anti-tumor drug development

Overexpression of $\alpha\beta_{III}$ has been associated with resistance to a wide range of chemotherapeutic drugs for several human malignancies. It has also been associated with drug sensitivity and tumor progression [7–10]. Out of the different αβ-tubulin isotypes, researchers have already

Table 2 Docking results (Glide XP) of noscapinoids with different αβ-tubulin isotypes

Docking score(kcal/mol)										
ISOTYPE	1	2	3	4	5	6	7	8	9	10
$\alpha\beta_{I}$	−5.278	−6.432	−5.601	−5.803	−5.213	−5.448	−5.039	−5.765	−6.328	−6.261
$\alpha\beta_{II}$	−6.671	−7.179	−6.897	−6.530	−6.851	−5.802	−6.327	−7.152	−7.147	−7.090
$\alpha\beta_{III}$	−5.278	−7.416	−7.242	−5.764	−5.496	−6.202	−5.151	−7.149	−7.126	−7.136
$\alpha\beta_{IV}$	−5.963	−7.317	−6.415	−6.617	−5.598	−3.084	−5.984	−6.312	−7.188	−6.364
$\alpha\beta_{V}$	−6.286	−5.453	−5.477	−6.270	−5.368	−6.280	−4.290	−6.086	−5.723	−6.792
$\alpha\beta_{VI}$	−5.903	−5.831	−5.763	−5.832	−6.560	−5.330	−7.148	−7.182	−7.010	−6.874
$\alpha\beta_{VII}$	−6.041	−6.351	−5.233	−6.506	−7.102	−4.547	−5.853	−7.136	−3.518	−6.371
$\alpha\beta_{VIII}$	−7.111	−6.804	−6.539	−6.068	−5.416	−5.706	−6.779	−7.236	−7.108	−7.205

All the noscapinoids bind well with different isotypes. However, each noscapinoid showed a different docking score with respect to different αβ-tubulin isotypes. Overall the amino-noscapine and the clinical derivative, bromo-noscapine showed better docking scores with the $\alpha\beta_{III}$-tubulin isotype in comparison to other isotypes

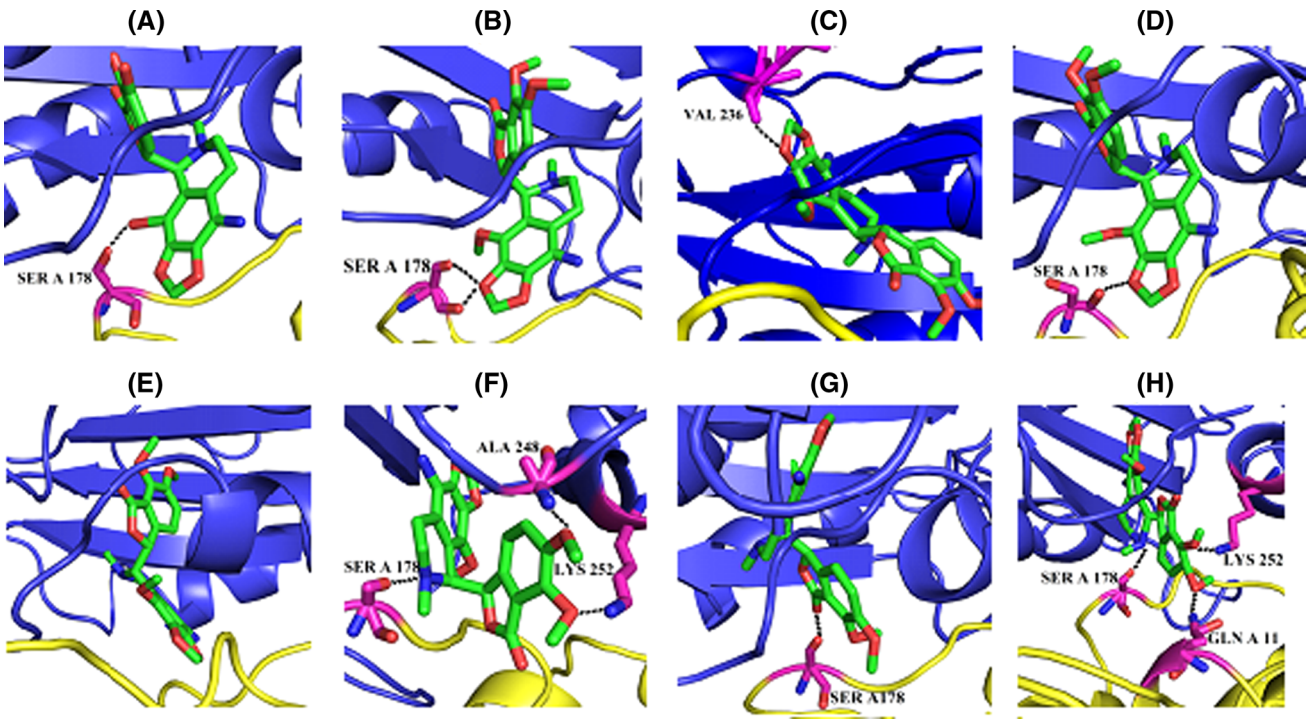

Fig. 4 The hydrogen bonding pattern revealed in the docking complexes of amino-noscapine with respect to **a** $\alpha\beta_{I}$-tubulin isotype, showing one hydrogen bond with Ser178 of α-chain; **b** $\alpha\beta_{II}$-tubulin isotype, showing two hydrogen bonds with Ser178 of α-chain; **c** $\alpha\beta_{III}$-tubulin isotype, showing one hydrogen bond with Val236 of β-chain; **d** $\alpha\beta_{IV}$-tubulin isotype, showing a hydrogen bond with Ser178 of α-chain; **e** $\alpha\beta_{V}$-tubulin isotype, showing no hydrogen bond with any of the chains; **f** $\alpha\beta_{VI}$-tubulin isotype, showing a hydrogen bond with Ser178 of α-chain, Ala248 and Lys252 of β-chain; **g** $\alpha\beta_{VII}$-tubulin isotype, showing a hydrogen bond with Ser178 of α-chain; **h** $\alpha\beta_{VIII}$-tubulin isotype, showing a hydrogen bond with Ser178 of α-chain, Gln11 of α-chain and Lys252 of β-chain

realized that $\alpha\beta_{III}$ would be an excellent target for anti-tumor drugs [14] and have used rational drug design to create a $\alpha\beta_{III}$-specific drug. The seco-taxoid, IDN 5390 [14] was explicitly designed to bind to the taxane binding site on $\alpha\beta_{III}$. This drug is very effective against paclitaxel resistant cell lines that overexpress $\alpha\beta_{III}$. To test whether the most potent noscapine derivative, amino-noscapine in our library and the clinical derivative, bromo-noscapine have a higher binding affinity with $\alpha\beta_{III}$-tubulin than noscapine, we narrowed our focus down to this isotype only. Targeting to $\alpha\beta_{III}$ by noscapinoids led to improvement of both efficacy and specificity of treatment. Both amino-noscapine and bromo-noscapine showed the highest docking score (Table 2) of −7.4 and −7.2 kcal/mol against this isotype in comparison to others. Paclitaxel and vinblastine which are both very successful in chemotherapy favour $\alpha\beta_{II}$ over $\alpha\beta_{III}$. They also suffer from side effects as $\alpha\beta_{II}$ is very abundant in the nervous system and a few other tissues. In contrast $\alpha\beta_{III}$ is less abundant in other tissues and has already been proven to be a very promising molecular target for cancer therapy. The ability of noscapinoids to target $\alpha\beta_{III}$ more specifically could be a reason for its unique properties in comparison to other tubulin binding agents.

Inspired by the docking result we determined the preferred binding mode and binding affinity of these two compounds and the lead compound noscapine with $\alpha\beta_{III}$ by performing 10 ns of MD simulation. The equilibration of the MD trajectories was monitored based on the convergence of plots of RMSDs of Cα carbon atoms of tubulin during 10 ns of MD simulation starting from the docked complex (Supplementary Figure S4). A total of 5,000 frames were generated for each molecular system out of which the last 1,000 frames were used to generate the average structure of the tubulin-drug complexes for the MM-GBSA and MM-PBSA calculation. The root mean square fluctuations (RMSF) of the residues within and around the noscapinoid binding site of $\alpha\beta_{III}$ in the free form and in complex with noscapinoids were also calculated to reveal the flexibility of these residues. Different levels of flexibility were noticed in the bound form of $\alpha\beta_{III}$ with different noscapinoids (Supplementary Figure S5). Most of the residues in the binding site showed flexibilities less than 2 Å in the case of $\alpha\beta_{III}$ when bound to noscapine, amino-noscapine and bromo-noscapine compared to free $\alpha\beta_{III}$. The RMSF of the bound form in comparison to the free form indicates that binding site residues become more rigid as a result of binding of the noscapinoids.

Binding affinity calculations

We found that all the three ligands fitted well into the binding site of $\alpha\beta_{III}$-tubulin isotype. In a representative example, the tight fit of amino-noscapine into the binding pocket of $\alpha\beta_{III}$-tubulin isotype is shown in Fig. 5. Further, the calculated binding free energy (ΔG_{bind}) and its components, based on MM-PBSA and MM-GBSA calculations, with $\alpha\beta_{III}$ (Table 3) indicated that amino-noscapine (−34.7 and −46.2 kcal/mol) bound more tightly than bromo-noscapine (−32.1 and −38.1 kcal/mol) and noscapine (−28.0 and −38.9 kcal/mol). Non polar solvation terms ($\Delta G_{sol\text{-}np}$), which correspond to the burial of solvent-accessible surface-area upon binding, contributes significantly to the binding of ligands. Similarly the intermolecular van der Waals (ΔE_{vdw}) also contributed significantly to the binding, whereas the polar solvation term ($\Delta G_{solv,PB(GB)}$) counteracted binding of these ligands. Although the gas-phase electrostatic value (ΔE_{gas}) favors the binding of the noscapinoids, the overall electrostatic interaction energy ($\Delta G_{ele,PB(GB)}$) is positive and thus unfavorable for the binding. This may be due to a large desolvation penalty of charged and polar groups that are not sufficiently compensated for by the complex formation.

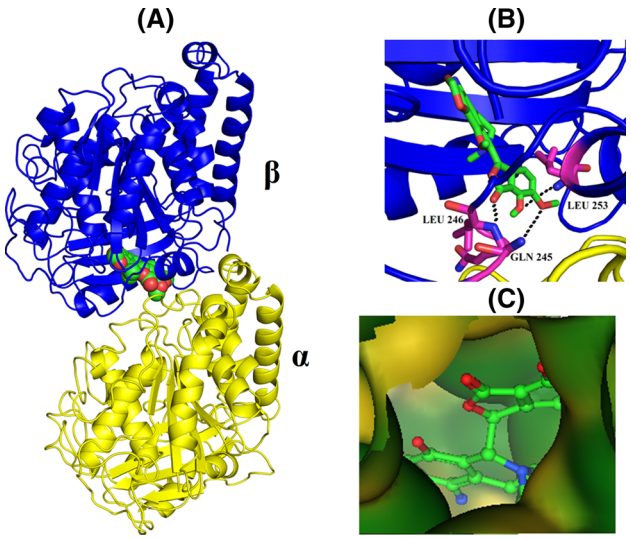

Fig. 5 Typical snapshot of binding mode of amino-noscapine with tubulin obtained after MD simulation. *Panel* (**a**) show the docked poses of amino-noscapine (space field) bound to $\alpha\beta_{III}$ at noscapine binding site. *Panel* (**b**) show the enlarged view the hydrogen bonding pattern of amino-noscapine with respect to $\alpha\beta_{III}$-tubulin isotype. Three hydrogen bonds contributing in the interaction of amino-noscapine with the binding site amino acids such as Gln245, Leu246 and Leu253 are shown in the figure. *Panel* (**c**) show the fitting of amino-noscapine with the binding site of $\alpha\beta_{III}$-tubulin isotype

Per residue energy contribution to noscapinoid binding

All the three ligands (noscapine, bromo-noscapine and amino-noscapine) were well accommodated into the binding site of $\alpha\beta_{III}$, at the interface between α- and β- tubulin, however, their binding interactions with the amino acids inside the binding cavity are distinct as shown in Fig. 6.

Table 3 Binding free energy (marked in bold) and its components (kcal/mol) for the receptor, $\alpha\beta_{III}$ heterodimer and noscapine derivatives

Energy components (kcal/mol)	Noscapine	Bromo-noscapine	Amino-noscapine
ΔE_{ele}	−325.4	−337.2	−348.8
ΔE_{vdw}	−56.22	−60.86	−57.42
ΔE_{gas}	−381.6	−398.0	−406.2
$\Delta G_{sol\text{-}np}$	−6.530	−6.120	−6.370
ΔG_{PB}	357.9	370.0	375.6
$\Delta G_{solv,PB}$	353.6	365.9	371.5
$\Delta G_{ele,PB}$	32.49	32.89	26.76
$\Delta G_{bind,\ PB}$	**−28.02**	**−32.05**	**−34.70**
ΔG_{GB}	349.3	366.0	366.4
$\Delta G_{solv,GB}$	342.7	359.9	360.0
$\Delta G_{ele,\ GB}$	23.87	28.88	17.52
$\Delta G_{bind,\ GB}$	**−38.86**	**−38.09**	**−46.23**

Per residue contribution of binding free energy is an efficient way to investigate the details of protein–ligand interactions at the atomic level. We have identified the residues that have the greatest impact, in terms of total energy (δG_{bind}) contribution (per residue contribution ≤ -1 kcal/mol), of the $\alpha\beta_{III}$ with the noscapinoids. For the binding of noscapine, residue Leu253 showed the largest contribution of ≤ -4 kcal/mol to the binding energy, while 9 other binding site residues (AlaA180, Ser239, Leu240, Leu246, Leu250, Asp256, Met257, Ala314 and Ile368) contributed energy ≤ -1 kcal/mol. For the binding of bromo-noscapine, residues Ala248 and Lys252 showed the largest contribution of ≤ -4 kcal/mol, whereas three other amino acids ThrA178, Val316 and Ala352 contributed ≤ -1 kcal/mol energy. Similarly, for amino-noscapine, Gln245, Leu253 and Leu246 showed largest contribution of ≈ -4 kcal/mol, while Ser239 and Leu240 contributed ≤ -2 kcal/mol energy.

To determine the detailed contribution of each important residue, the summations of the per residue interaction free energy (δE_{total}) was split into van der Waals (δE_{vdw}), electrostatic (δE_{elec}) and polar solvation ($\delta E_{sol,GB}$) energies. The energy contributions from the selected residues are shown in Supplementary Figure S6. In the $\alpha\beta_{III}$-noscapine complex, Leu253 has significant δE_{elec} contribution energy (≤ -5 kcal/mol), leading to formation of one H-bond (Table 4). However, for $\alpha\beta_{III}$-bromo noscapine complex, two amino acids such as Ala248 and Lys252 have appreciable δE_{elec} contribution energy (≤ -5 kcal/mol), leading to formation of two H-bonds (Table 4), while Leu253 has the strongest attraction interaction (with $\delta E_{vdw} \leq -3.4$ kcal/mol) with bromo-noscapine. Similarly, for $\alpha\beta_{III}$-amino noscapine complex, three amino acids such as Gln245, Leu246 and Leu253 have maximum δE_{elec} energy contribution (≤ -5 kcal/mol), leading to formation

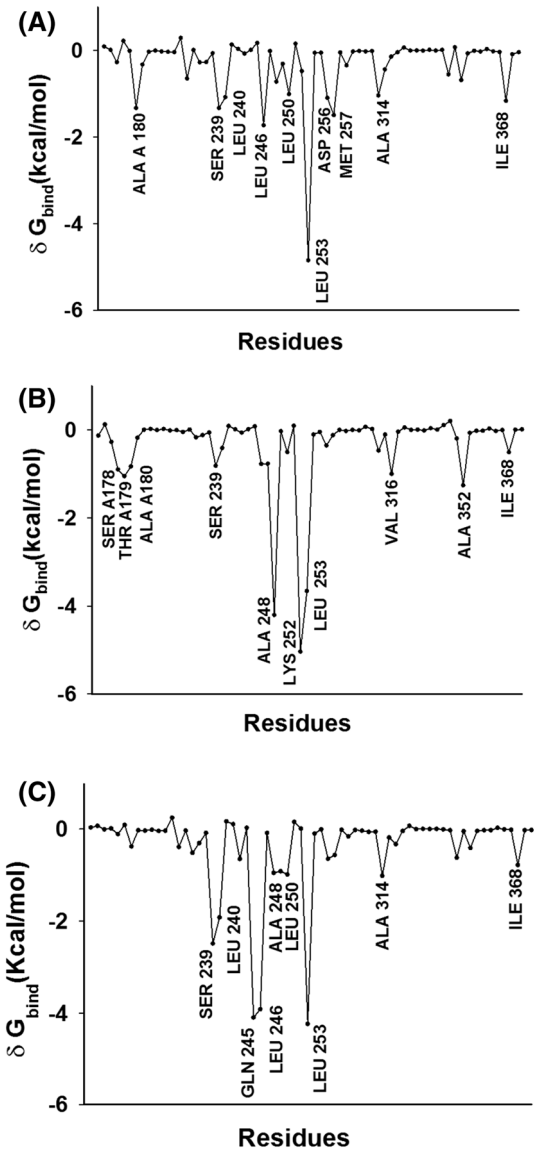

Fig. 6 Per residue binding free energy (δG_{bind}) contribution of $\alpha\beta_{III}$ for the binding of **a** noscapine, **b** bromo-noscapine and **c** amino-noscapine. Only the amino acids within 12 Å of the binding site were considered

Table 4 Hydrogen bonding (H-bond) patterns between the residues of $\alpha\beta_{III}$ with amino-noscapine, bromo-noscapine and noscapine

Donor	Acceptor	Distance (Å)
Amino noscapine		
GlnB245 N2	Lig O25	2.7
LeuB246N	Lig O23	3.4
Leu B253N	Lig O24	2.8
Bromo noscapine		
AlaB248N	Lig O23	2.84
LysB252 N2	Lig O24	3.66
Noscapine		
LeuB253N	Lig O23	2.78

of three H-bonds (Table 4), while Ser239 contributed better δE_{vdw} energy (≤ -2.7 kcal/mol) with amino-noscapine. The results also revealed that most of the residues while binding to the noscapinoids showed a minor contribution in δE_{vdw} energy (≤ -1.0 kcal/mol).

Conclusion

The computational data paves a way to correlate the differential responses of noscapinoids against the cancer cells of different tissue of origin in the context of binding pattern of noscapinoids with respect to different αβ-tubulin isotypes. We have provided three lines of evidence to support this hypothesis: (1) All-vs-all comparison of the amino acids constituting the noscapinoid binding site and within 12 Å diameter showed significant variations among the isotypes. The differences in conformation and composition of binding site amino acids suggest differences in the overall environment of the binding site that may affect the binding affinity of noscapinoids. (2) The differential binding affinity and mode of interaction of noscapinoids from docking experiment suggests different specificity of noscapinoids across different αβ-tubulin isotypes. (3) Amino-noscapine and bromo-noscapine specifically showed highest binding affinity with $\alpha\beta_{III}$-tubulin (an important target associated with resistance to a wide range of chemotherapeutic drugs) as calculated by MM-PBSA and MM-GBSA methods. The ability of noscapinoids to specifically target $\alpha\beta_{III}$ could explain their unique properties in comparison to other tubulin binding agents such as paclitaxel and vinblastine which favour $\alpha\beta_{II}$ over $\alpha\beta_{III}$. Taken together, targeting to different αβ-tubulin isotypes by noscapinoids may lead to improvement of both efficacy and specificity of cancer treatments in different tissues.

Acknowledgments Authors are thankful to Dr. Harish Joshi, School of Medicine, Emory University, Georgia, USA, for carefully reading the manuscript and for providing constructive criticism. We are greatly indebted to the anonymous reviewers of this manuscript for their helpful suggestions.

References

1. Stanton RA, Gernert KM, Nettles JH, Aneja R (2011) Drugs that target dynamic microtubules: a new molecular perspective. Med Res Rev 31(3):443–481
2. Checchi PM, Nettles JH, Zhou J, Snyder JP, Joshi HC (2003) Microtubule-interacting drugs for cancer treatment. Trends Pharmacol Sci 24(7):361–365
3. Downing KH (2000) Structural basis for the interaction of tubulin with proteins and drugs that affect microtubule dynamics. Annu Rev Cell Dev Biol 16:89–111
4. Alam MA, Naik PK (2009) Molecular modelling evaluation of the cytotoxic activity of podophyllotoxin analogues. J Comput Aided Mol Des 23:209–225
5. Luduena RF (1998) Multiple forms of tubulin: different gene products and covalent modifications. Int Rev Cytol 178:207–275
6. Banerjee A, Luduena RF (1992) Kinetics of colchicine binding to purified beta tubulin isotypes from bovine brain. J Biol Chem 267:13335–13339
7. Mozzetti S, Ferlini C, Concolino P et al (2005) Class III B-tubulin overexpression is a prominent mechanism of paclitaxel resistance in ovarian cancer patients. Clin Cancer Res 11:298–305
8. Joshua A, McCarroll Gan PP, Liu M, Kavallaris M (2010) βIII-tubulin is a multifunctional protein involved in drug sensitivity and tumorigenesis in non-small cell lung cancer. Clin Cancer Res 70(12):4995–5003
9. Nicoletti MI, Valoti G, Giannakakou P et al (2001) Expression of β_tubulin isotypes in human ovarian carcinoma xenografts and in a sub-panel of human cancer cell lines from the NCI-anticancer drug screen: correlation with sensitivity to microtubule active agents. Clin Cancer Res 7:2912–2922
10. Zhang Y, Yang H, Liu J et al (2013) High expression levels of class III β-tubulin in resected non-small cell lung cancer patients are predictive of improved patient survival after vinorelbine-based adjuvant chemotherapy. Oncol Lett 6:220–226
11. Huzil JT, Luduena RF, Tuszynski J (2006) Comparative modelling of human beta-tubulin isotypes and implications for drug binding. Nanotechnology 17:S90–S100
12. Mane JY, Klobukowski MJ, Huzil T, Tuszynski J (2008) Free energy calculations on the binding of colchicine and its derivatives with the α/β-tubulin isoforms. J Chem Inf Model 48(9):1824–1832
13. Gan PP, Pasquier E, Kavallaris M (2000) Class III beta-tubulin mediates sensitivity to chemotherapeutic drugs in non small cell lung cancer. Cancer Res 67:9356–9363
14. Kim YS, Tseng CY, Mane JY, Winter P, Johnson L, Huzil T, Izbicka E, Luduena RF, Tuszynski J (2010) Quantitative analysis of the effect of tubulin isotype expression on sensitivity of cancer cell lines to a set of novel colchicine derivatives. Mol Cancer 9:131
15. Christoph DC, Kasper S, Gauler TC, Loesch C, Engelhard M, Theegarten D, Poettgen C, Hepp R, Peglow A, Loewendick H, Welter S, Stamatis G, Hirsch FR, Schuler M, Eberhardt WE, Wohlschlaeger J (2012) βV-tubulin expression is associated with outcome following taxane-based chemotherapy in non-small cell lung cancer. Br J Cancer 107:823–830
16. Ye K, Ke Y, Keshava N, Shanks J, Kapp JA, Tekmal RR, Petros J, Joshi HC (1998) Opium alkaloid noscapine is an antitumor agent that arrests metaphase and induces apoptosis in dividing cells. Proc Natl Acad Sci USA 95:1601–1606
17. Joshi HC, Salil A, Bughani U, Naik PK (2010) Noscapinoids: a new class of anticancer drugs demand bio-technological intervention. In: Arora R (ed) Medicinal plant biotechnology, CAB e-Books CABI (H ISBN 9781845936785)
18. Mahmoudian M, Rahimi-Moghaddam P (2009) The anti-cancer activity of noscapine: a review. Recent Pat Anticancer Drug Discov 4(1):92–97
19. Landen J, Lang WR, McMahon SJ, Rusan NM, Yvon AM, Adams AW, Sorcinelli MD, Campbell R, Bonaccorsi P, Ansel JC, Archer DR, Wadsworth P, Armstrong CA, Joshi HC (2002) Noscapine alters microtubule dynamics in living cells and inhibits the progression of melanoma. Cancer Res 62:4109–4114
20. Zhou J, Panda D, Landen JW, Wilson L, Joshi HC (2002) Minor alteration of microtubule dynamics causes loss of tension across kinetochore pairs and activates the spindle checkpoint. J Biol Chem 277:17200–17208
21. Aneja R, Vangapandu SN, Lopus M, Viswesarappa VG, Dhiman N, Verma A, Chandra R, Panda D, Joshi HC (2006) Synthesis of microtubule-interfering halogenated noscapine analogues that

perturb mitosis in cancer cells followed by cell death. Biochem Pharmacol 72:415–426
22. Zhou J, Gupta K, Aggarwal S, Aneja R, Chandra R, Panda D, Joshi HC (2003) Brominated derivatives of noscapine are potent microtubule-interfering agents that perturb mitosis and inhibit cell proliferation. Mol Pharmacol 63:799–807
23. Aneja R, Vangapandu SN, Lopus M, Chandra R, Panda D, Joshi HC (2006) Development of a novel nitro-derivative of Noscapine for the potential treatment of drug-resistant ovarian cancer and Tcell lymphoma. Mol Pharmacol 69:1801–1809
24. Naik PK, Chatterji BP, Vangapandu SN, Aneja R, Chandra R, Kanteveri S, Joshi HC (2011) Rational design synthesis and biological evaluations of amino-noscapine: a high affinity tubulin-binding noscapinoids. J Comput Aided Drug Des 25:443–454
25. Zhou J, Gupta K, Yao J, Ye K, Panda D, Giannakakou P, Joshi HC (2002) Paclitaxel-resistant human ovarian cancer cells undergo v-Jun NH_2-terminl kinase-mediated apoptosis in response to noscapine. J Biol Chem 277(42):39777–39785
26. Santoshi S, Naik PK, Joshi HC (2011) Rational design of novel anti-microtubule agent (9-azido-noscapine) from quantitative structure activity relationship (QSAR) evaluation of noscapinoids. J Biomol Screen 16:1047–1058
27. Manchukonda NK, Naik PK, Santoshi S, Lopus M, Joseph S, Sridhar B, Kantevari S (2013) Rational design synthesis and biological evaluation of third generation α-noscapine analogues as potent tubulin binding anti-cancer agents. PLoS ONE 8(10):77970
28. Naik PK, Santoshi S, Rai A, Joshi HC (2011) Molecular modelling and competition binding study of Br-noscapine and colchicine provide insight into noscapinoid-tubulin binding site. J Mol Graph Model 29:947–955
29. Hall TA (1999) BioEdit: a user-friendly biological sequence alignment editor and analysis program for Windows 95/98/NT. Nucleic Acids Symp Ser 41:95–98
30. Berendsen HJC, Spoel VD, Drunen VR (1995) GROMACS: a message passing parallel molecular dynamics implementation. Comput Phys Commun 91:43–56
31. Daren T, York D, Pedersen L (1993) Particle mesh Ewald: an N-log(N) method for Ewald sums in large systems. J Chem Phys 98:10089–10092
32. Hess B, Bekker H, Berendsen HJC, Fraaije JGEM (1997) LINCS: a linear constraint solver for molecular simulations. J Comput Chem 18:1463–1472
33. Laskowski RA, MacArthur MW, Moss DS, Thornton JM (1993) PROCHECK: a program to check the stereochemical quality of protein structures. J App Crystal 26:283–291
34. Ramachandran GN, Ramakrishnan C, Sasisekharan V (1963) Stereochemistry of polypeptide chain configurations. J Mol Biol 7:95–99
35. Colovos C, Yeates TO (1993) Verification of protein structures: patterns of non-bonded atomic interactions. Protein Sci 2:1511–1519
36. Eisenberg D, Luthy R, Bowie JU (1997) VERIFY3D: assessment 694 of protein models with three-dimensional profiles. Methods Enzymol 277:396–404
37. Lee C, Yang W, Parr RG (1988) Development of the Colle-Salvetti correlation-energy formula into a functional of the electron density. Phys Rev B 37:785–789
38. Becke AD (1993) A new mixing of Hartree-Fock and local density-functional theories. J Chem Phys 98:1372–1377
39. Binkley JS, Pople JA, Hehre WJ (1980) Self-consistent molecular orbital methods 21 small split-valence basis sets for first-row elements. J Am Chem Soc 102:939–947
40. Gordon MS, Binkley JS, Pople JA, Pietro WJ, Hehre WJ (1982) Self-consistent molecular-orbital methods 22 small split-valence basis sets for second-row elements. J Am Chem Soc 104:2797–2803
41. Pietro WJ, Francl MM, Hehre WJ, Defrees DJ, Pople JA, Binkley JS (1982) Self-consistent molecular orbital methods 24 supplemented small split-valence basis sets for second-row elements. J Am Chem Soc 104:5039–5048
42. Friesner RA, Banks JL, Murphy RB, Halgren TA, Klicic JJ, Mainz DT, Repasky MP, Knoll EH, Shelley M, Perry JK, Shaw DE, Francis P, Shenkin PS (2004) Glide: a new approach for rapid accurate docking and scoring 1 method and assessment of docking accuracy. J Med Chem 47:1739–1749
43. Halgren TA, Murphy RB, Friesner RA, Beard HS, Frye LL, Pollard WT, Banks JL (2004) Glide: a new approach for rapid accurate docking and scoring 2 enrichment factors in database screening. J Med Chem 47:1750–1759
44. Case DA, Walker RC et al (2010) AMBER 11. University of California, San Francisco
45. Cornell WD, Cieplak P, Bayly CI, Gould IR, Merz KM Jr, Ferguson DM, Spellmeyer DC, Fox T, Caldwell JW, Kollman PA (1995) A second generation force field for the simulation of proteins nucleic acids and organic molecules. J Am Chem Soc 117:5179–5197
46. Wang JM, Wolf RM, Caldwell JW, Kollamn PA, Case DA (2004) Development and testing of a general amber force field. J Comput Chem 25:1157–1174
47. Ryckaert JP, Ciccotti G, Berendsen HJC (1977) Numerical integration of the Cartesian equations of motion of a system with constraints: molecular dynamics of n-alkanes. J Comput Phys 23:327–341
48. Hornak V, Abel R, Okur A, Strockbine B, Roitberg A, Simmerling C (2006) Comparison of multiple Amber force fields and development of improved protein backbone parameters. Protein 65:712–725
49. Berendsen HJC, Postma JP, van Gunsteren WF, DiNola A, Haak JR (1984) Molecular dynamics with coupling to an external bath. J Chem Phys 81:3684–3691
50. Kollman PA, Massova I, Reyes C, Kuhn B, Huo S, Chong L, Lee M, Lee T, Duan Y, Wang W, Donini O, Cieplak P, Srinivasan J, Case DA, Cheatham TE (2000) Calculating structures and free energies of complex molecules: combining molecular mechanics and continuum models. Acc Chem Res 33:889–897
51. Shen XL, Kamimura MT, Wei J, Gao QZ (2012) Computer-aided de novo ligand design and docking/molecular dynamics study of vitamin D receptor agonists. J Mol Model 18:203–212
52. Niu X, Gao X, Wang H, Wang X, Wang S (2013) Insight into the dynamic interaction between different flavonoids and bovine serum albumin using molecular dynamics simulations and free energy calculations. J Mol Model 19:1039–1047
53. Guo J, Wang X, Sun H, Liu H, Yao X (2012) T he molecular basis of IGF-II/IGF2R recognition: acombined molecular dynamics simulation free-energy calculation and computational alanine scanning study. J Mol Model 18:1421–1430